

Diffraction and Dynamic Stress Concentration around Multiple Holes in a Finite Elastic Solid by BEM

S. Parvanova¹, P. Dineva² and G. Manolis³

Abstract: The aim of the present study is to develop and validate an efficient boundary element method approach for solution of in-plane, time-harmonic problems in elastodynamics that involve finite elastic solids weakened by holes of different shapes. The modeling approach is within the framework of continuum mechanics and linear wave propagation theory. The results obtained show a sensitivity of both the dynamic stress concentration factor and the scattered wave field that develop in the finite solid to defect geometry, to wave interaction with the holes and to multiple hole interaction.

Keywords: Diffraction, stress concentration, cavities, in-plane elastic waves, BEM.

1 Introduction

Elastic wave propagation in solids weakened by multiple cavities (or defects) is an old problem of mechanics [Mow and Mente (1963); Pao and Mow (1971)] with extensive applications in many modern technological fields such as material science, non-destructive testing evaluation and computational geophysics [Hirose (1989); Manolis (2003); Meguid and Wang (1995)]. A clear understanding of both the wave scattered far-field and the dynamic stress concentration factor (SCF) around holes provides useful information for predicting the life expectancy of various engineering structures, new technological devices and even underground structures such as tunnels or pipelines. The present work is an effort in this direction that aims to develop and validate an efficient boundary element method (BEM) approach, which in turn can be used for solving in-plane, time-harmonic problems involving a finite elastic solid with holes of different shapes (e.g., square, circular or elliptic).

¹ University of Architecture, Civil Engineering and Geodesy (UACEG), 1046 Sofia, Bulgaria

² Institute of Mechanics, Bulgarian Academy of Sciences (BAS), 1113 Sofia, Bulgaria

³ Department of Civil Engineering, Aristotle University (AUTH), 54124 Thessaloniki, Greece

2 Problem statement and its BEM formulation

Consider a finite homogeneous linear elastic solid with boundary Γ in a Cartesian coordinate system $Ox_1x_2x_3$. The solid is subjected to a time-harmonic load with prescribed frequency ω . The analysis is then carried out for in-plane motion with respect to plane $x_3 = 0$. The nonzero field quantities are the displacements u_1, u_2 and the stresses $\sigma_{11}, \sigma_{22}, \sigma_{12}$, all depending on (x_1, x_2) . Since the response is also time-harmonic, the common multiplier $\exp(i\omega t)$ is suppressed in the following. Next, the field equations in the absence of body forces are given by:

$$\sigma_{ij,j} + \rho \omega^2 u_i = 0 \quad (1)$$

where ρ is the material density, $\sigma_{ij} = C_{ijkl}u_{k,l}$, $C_{ijkl} = \lambda \delta_{ij}\delta_{kl} + \mu(\delta_{ik}\delta_{jl} + \delta_{il}\delta_{jk})$, δ_{ij} is the Kronecker delta symbol and λ, μ are the Lamé constants. Subscript commas denote partial differentiation and the summation convention over repeated indices is applied. The solid contains multiple circular holes Γ_h^m , $m = 1, 2, \dots, M$ of diameter d and center C_h^m , quadratic holes with size a , or ellipsoidal holes with semi-axes $d_1/2$ and $d_2/2$. We assume the holes do not intersect and denote their total surface as $\Gamma_h = \bigcup_{k=1}^M \Gamma_h^m$. The boundary conditions along the solid's outer boundary Γ are prescribed displacements $u_i(x_1, x_2) = \bar{u}_i(x_1, x_2)$ on Γ_u or/and tractions $t_i(x_1, x_2) = \sigma_{ij}n_j = \bar{t}_i(x_1, x_2)$ on Γ_t , where $\Gamma = \Gamma_u \cup \Gamma_t$. The hole surfaces are traction-free as $t_i^m(x_1, x_2) = 0$, $(x_1, x_2) \in \Gamma_h^m$ and the total problem boundary is $S = \Gamma \cup \Gamma_h$.

An equivalent formulation to the above boundary-value problem (BVP) is a system of boundary integral equations (BIE) along hole boundaries Γ_h plus the external boundary Γ . This yields the conventional displacement BEM, see Manolis and Beskos (1981):

$$c_{ij}u_j(\mathbf{x}, \omega) = \int_s U_{ij}^*(\mathbf{x}, \mathbf{y}, \omega)t_j(\mathbf{y}, \omega) ds - \int_s P_{ij}^*(\mathbf{x}, \mathbf{y}, \omega)u_j(\mathbf{y}, \omega) ds \quad (2)$$

where c_{ij} is the jump term depending on the geometry at the collocation point, $\mathbf{x} = (x_1, x_2)$ and $\mathbf{y} = (y_1, y_2)$ are the position vectors of the field and source points, U_{ij}^* is the fundamental solution of Eq. 1 and P_{ij}^* is the corresponding traction solution.

3 Numerical procedure, validation and parametric study

3.1 BEM discretization and validation study

The numerical procedure is based on discretization of the boundary S by line elements, followed by nodal collocation. After satisfaction of the boundary conditions, the BIE transforms into a system of linear algebraic equations with respect

to the unknown displacement and/or tractions. Curved geometries can be successfully represented by quadratic or higher order line elements; the former types of elements are employed here.

A MATLAB software code for 2D problems has been developed based on the theory described above and on the FORTRAN source codes given by Domínguez (1993). This program allows for traction values assigned on both sides of a given node, connecting two elements, to be different. In addition, provisions are made for modeling of several closed domains.

In sum, many numerical examples and comparisons with exact analytical solutions have been worked out that show excellent accuracy of the developed software code with solutions given in the literature. Some additional comparisons have been performed with general purpose software programs based on the finite element method (FEM). The BEM models, realized by using relatively coarse meshes, have shown superb accuracy when compared with corresponding FEM solutions.

3.2 Parametric study

In the interest of brevity, the results of a single parametric study are given in this paper that investigate the effect of cavity shape on the scattered wave field, together with the dynamic hole interaction phenomenon. Conclusions are drawn by monitoring a typical displacement of node A from the outer boundary of the finite region, and the stress concentration factor for node B on the surface of a circular or elliptic cavity (see Fig. 1).

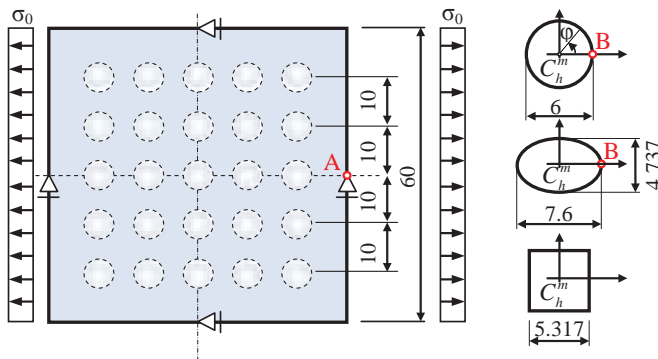


Figure 1: Geometrical dimensions of the perforated plate under tension

The solid matrix is a square plate whose dimensions, boundary conditions, external loads, and potential locations of the holes are all given in Fig. 1. The mechanical properties of the plate are: density $\rho = 0.5 \times 10^{-5} \text{kg/mm}^3$; shear modulus $G =$

$0.76923 \times 10^5 N/mm^2$; Poisson's ratio $\nu = 0.3$, and plate size $60 \times 60 mm$. The amplitude of the time-harmonic load is $\sigma_0 = 400 N/mm^2$. In order to restrict rigid body motion in the x_1 direction, nodes belonging to the vertical axis of symmetry are restrained, and so are the vertical displacements of nodes on the horizontal axis of symmetry.

The shape of a given cavity can be circular, elliptic or square. More specifically, the radius of a circle is $d/2 = 3 mm$, while the first semi-axis an ellipse is $d_1/2 = 3.8$, the second semi-axis is $d_2/2$, and both are calculated so that the area of the elliptical cavity equals to the area of the circular one (see Fig. 1). The size of the square is again determined so that its area equals to the circular one.

Next, the numerical model is shown in Fig. 2. The outer contour is discretized by using 16 equal-length quadratic elements, 4 along each side of the square. Each single hole is modeled by 8 quadratic elements, independently of its shape. In order to properly define the outer plate domain in the BEM discretization, the interface must be traversed in a counter-clockwise direction; conversely, the cavity contour must be discretized in the clockwise direction.

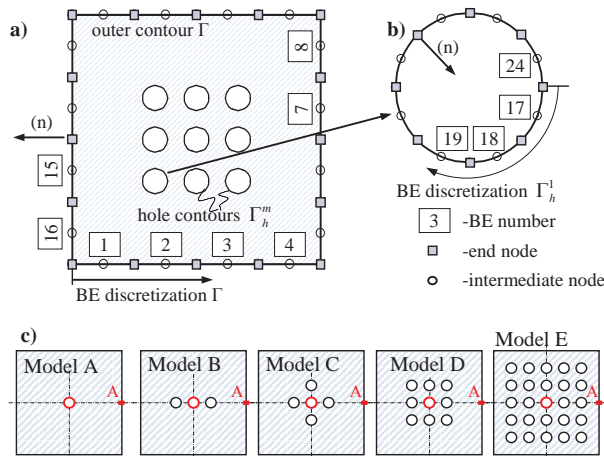


Figure 2: BEM model: a) BE discretization of the plate domain; b) BE mesh of the cavity contour; c) Hole arrangement for different cases

The dimensionless excitation frequency for a given value of the P-wave velocity C_p ranges from $\Delta\Omega = (\omega \times (2a)/C_p)/40$ to $\Omega = \omega \times (2a)/C_p = 1$ in 40 equal increments, where a is a characteristic dimension of the cavity. This characteristic dimension for a circle is obviously the diameter $a = d$; $a = (d_1 + d_2)/2$ for elliptic holes; a is the side for square holes.

In the parametric study two key values are tracked, namely the horizontal displacement at node A on the outer boundary and the stress concentration factor (SCF) at point B of a circular and elliptic contour at point B (see Fig. 2). The reference hole is always the same, placed at the center of the square plate and marked in red (see Fig. 3c). The amplitude of the load is $\sigma_0 = 400$, and the SCF is the value of the hoop stress at the monitored node $\sigma_{\theta\theta}$ normalized by σ_0 .

The results for the circular holes are given in Fig. 3. More specifically, the normalized displacement as obtained from the different configurations shown in Fig. 2c, versus normalized frequency, is depicted in Fig. 3a. In there, the horizontal displacement of node A at the outer contour is normalized by the corresponding displacement obtained from the same plate in the absence of holes, namely u_0 . The SCF at B is then shown in Fig. 3b.

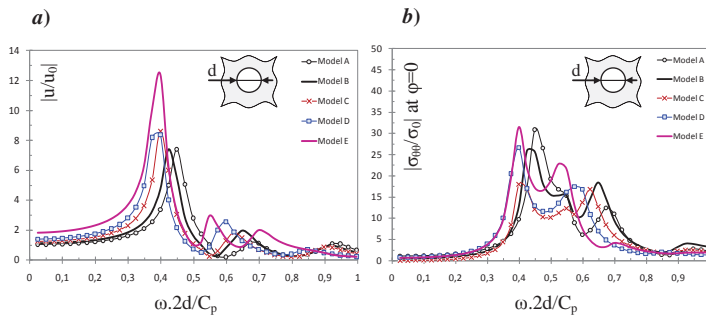


Figure 3: a) Normalized displacement spectra; b) Steady-state SCF response of the circular hole at $\varphi = 0^\circ$.

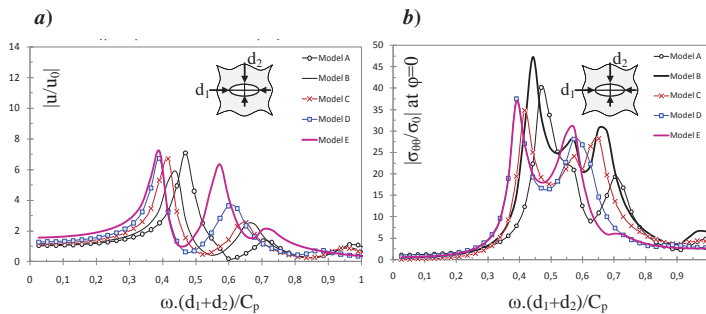


Figure 4: a) Normalized displacement spectra; b) Steady-state SCF response of the elliptic hole at $\varepsilon = 0^\circ$

The normalized displacement and SCF versus normalized frequency for the elliptic hole are all plotted in Fig. 4. As expected, the SCF is larger than the corresponding value for the circular hole because of the sharper curvature at point B, whereas the displacement is smaller.

Finally, the square hole displacement curves are plotted in Fig. 5.

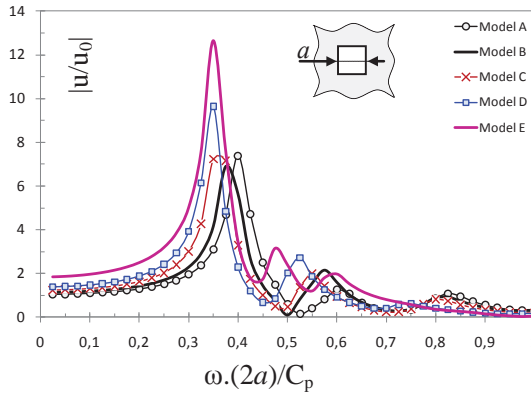


Figure 5: Normalized displacement spectra for the solid with square holes.

4 Conclusion

The 2D elastodynamic problem for a solid containing an arbitrary number of holes with different shape and position is solved in frequency domain. The results reveal the sensitivity of both the dynamic stress concentrations and scattered wave field to hole geometry, their number and position, and their interaction with the incoming wave.

Acknowledgement: The MC-IEF grant No. PIEF-GA-2010-270889 is acknowledged.

References

Domínguez, J. (1993): *Boundary Elements in Dynamics*. Elsevier Applied Science, New York.

Hirose, S. (1989): Scattering from an elliptic crack by the time-domain boundary integral equation method. In Brebbia CA, C. J.(Ed): *Advances in Boundary Elements: Stress Analysis*, pp. 99–110, Berlin. Springer-Verlag.

Manolis, G. D. (2003): Elastic wave scattering around cavities in inhomogeneous continua by the bem. *J. Sound and Vibration*, vol. 266, pp. 281–305.

Manolis, G. D.; Beskos, D. E. (1981): Dynamic stress concentration studies by boundary integrals and laplace transform. *Int. J. Num. Meth. Engng.*, vol. 17, pp. 573–599.

Meguid, S. A.; Wang, X. D. (1995): The dynamic interaction of a crack with a circular hole under anti-plane loading. *J. Mech. Phys. Solids*, vol. 43, no. 12, pp. 1857–1874.

Mow, C. C.; Mente, L. J. (1963): Dynamic stresses and displacements around cylindrical discontinuities due to plane harmonic shear waves. *J. Appl. Mech.*, vol. 30, pp. 598–604.

Pao, Y. H.; Mow, C. C. (1971): *Diffraction of Elastic Waves and Dynamic Stress Concentration*. Crane Russak, New York.

